Original paper

Origin of V–Cr–Ti-mineralization in thermally overprinted metal-rich black shales from the Teplá–Barrandian Unit (Bohemian Massif) and implications for metal remobilization during metamorphism

František VESELOVSKÝ[1]*, Jan PAŠAVA[1], Ondřej POUR[1], Lukáš ACKERMAN[2]

[1] *Czech Geological Survey, Klárov 3, 118 21 Prague 1, Czech Republic; frantisek.veselovsky@geology.cz*
[2] *Institute of Geology of the Czech Academy of Sciences, Rozvojová 269, 165 00 Prague 6, Czech Republic*
* *Corresponding author*

We present a detailed study of geochemical composition and ore mineralogy of black shales from Chynín, Czech Republic, representing Ediacaran organic matter-rich sediments, which were subject to regional and contact metamorphism. They are part of the Blovice Accretionaly Complex (BAC) in the Teplá–Barrandian Unit (TBU) and are located close to the contact with the Central Bohemian Pluton (CBP). The black shales were encountered with metasilicites, metabasalts, and basic tuffitic rocks in the CHY-2 drill hole (250 m deep) and are regionally associated with hornfels bodies. The geochemistry of these shales indicates that they correspond to metal-rich black shales deposited under strongly reducing conditions (TOC/P_{molar} > 100, high Mo and U values). On the other hand, the lack of a positive link between TOC and redox-sensitive metals (e.g., V, U, Cr, Ni, Mo) and their generally negative correlation with sulfur indicate important late-stage metal and sulfur remobilization. This is reflected in the mineralogical composition of the shales, which documents a thermal event in their history. Abundant framboidal pyrite (pyrite I) was recrystallized into coarse aggregates (pyrite II), locally accompanied by chalcopyrite, sphalerite, and rare molybdenite, pentlandite and breithauptite. Abundant pyrrhotite formed there due to selective desulfurization of pyrite I and II during the contact metamorphism. Locally, this process was also accompanied by the replacement of pyrrhotite by V–Cr–O (karelianite – V_2O_3 and eskolaite – Cr_2O_3, mostly with dominant karelianite end-member) and Ti–V–O (vanadium rutile, schreyerite – $V_2Ti_3O_9$ and a phase with the theoretical composition $V_4Ti_3O_{12}$, yet unknown to the mineralogical system). Vanadium–Cr–Ti elemental associations reported from different localities of Neoproterozoic metal-rich black shales, metal-rich black shales, and (meta)silicites in TBU indicate similar sources of these elements but different conditions of their accumulation.

1. Introduction

The close association of metal-rich black shales with cherts, volcanogenic rocks and other lithologies have been reported from various geotectonic settings in many geological terranes; these facies may locally become a source of precious and base metals, as well as U, V, Mo, Ni, Mn, Hg, Sb, and W (Fan 1983; Coveney and Glascock 1989; Oszczepalski 1989; Grauch and Huyck 1990; Coveney and Chen 1991; Loukola-Ruskeeniemi 1991; Leventhal 1993; Pašava 1993; Wignall 1994; Pašava et al. 1996; Loukola-Ruskeeniemi 1999; Coveney 2000; Pašava et al. 2003; Coveney and Pašava 2004; Polgári et al. 2012; Lehmann et al. 2016 and others).

Yudovich and Ketris (1994) reported global median values of V (200 ± 10 ppm, *n* = 25207) and Cr (93 ± 3 ppm, *n* = 21900) in black shale, showing much higher V-enrichment than Cr. These values are comparable with those of low-grade metamorphosed Neoproterozoic black shales of the Teplá–Barrandian Unit (TBU) (V = 212 ppm, Cr = 93 ppm, *n* = 47) (Pašava 2000) in which V correlates with total organic carbon (TOC), while Cr is significantly linked with organic matter and sulfur only locally. Loukola-Ruskeeniemi and Lahtinen (2012) reported 545 ppm V and 129 ppm Cr in Paleoproterozoic Talvivaara black schists (part of the Kainu schist belt, Finland) that were metamorphosed to greenschist-amphibolite facies (Loukola-Ruskeeniemi and Lahtinen 2012) and noticed a weak correlation between TOC and V (which they explained in terms of bottom waters being anoxic/euxinic). Uranium-rich Cambrian Alum shale (Southern Storsjön area, Sweden) has on average 1600 ppm V and 112 ppm Cr, while the Average Cambrian Alum shale contains 680 ppm V and 94 ppm Cr (Upper member) and 450 ppm V (Middle and Lower members) (Andersson et al. 1985). In general, V concentrations in the Cambrian Alum shale are closely associated with organic matter (Bian et al. 2021).

Vanadium ore beds associated with black shales in the South China Block consist of black silty shales, cherts, and phosphatic nodular shales and reach thicknesses between 10 and 20 m. Vanadium is primarily incorporated
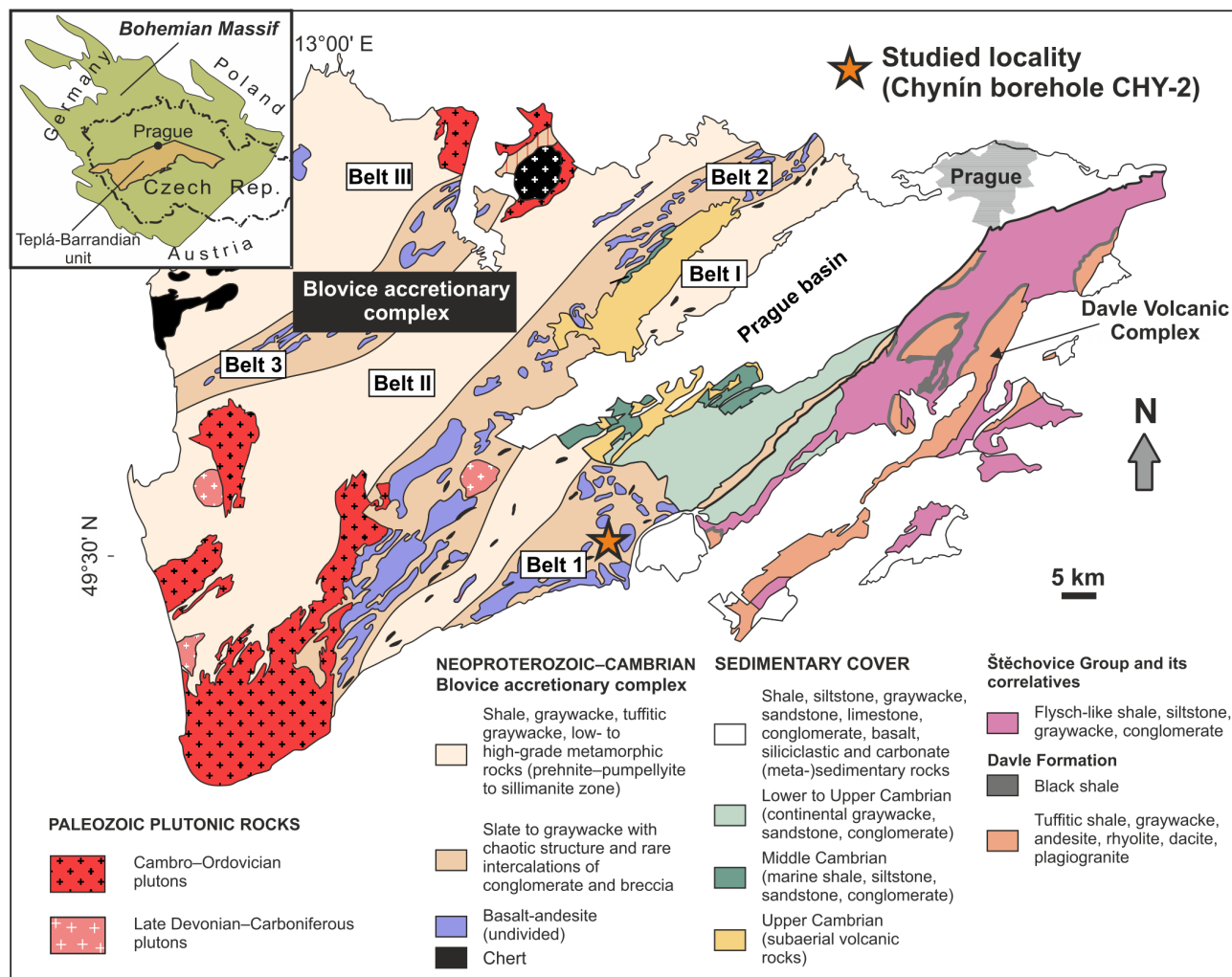
Fig. 1 Geological map of the Teplá–Barrandian Unit (adopted and modified from Hajná et al. 2019) with the studied Chynín locality marked.

in vanadian illite and is uniform in content throughout the beds (1–2 wt. % V_2O_3; Chen et al. 1990). Metalliferous black slates from the Late Proterozoic to Palaeozoic Okcheon Metamorphic Belt (Korean Peninsula) bearing up to 2.04 wt. % V and 0.33 wt. % Cr, represent metamorphosed analogs of the Early Cambrian V–Ba deposits hosted by the black shales in the South China Block. Vanadium garnet goldmanite – $Ca_3V^{3+}_2(SiO_4)_3$ occurs locally as porphyroblasts (Jeong 2006). The Mecca Quarry Shale Member of upper Carboniferous age (USA) contains 210–3880 ppm V and 280–780 ppm Cr (Coveney et al. 1987). Vanadium occurs in solid solution within illite-rich illite–smectite (I–S), having an average content of 1.65 wt. % V, and overall composition of $K_{0.8}(Al_{2.8}Mg_{0.5}Fe_{0.4}V_{0.3})(Si_{7.2}Al_{0.8})O_{20}(OH)_4$ analogous to the V-rich dioctahedral mica, roscoelite (Peacor et al. 2000). Vanadiferous horizons in the Meade Peak member represented by black shale and mudstone within the Phosphoria Formation of Permian age (USA) grade on average from 0.7 to 1.6 wt. % V_2O_5 (Love 1967).

Under strongly reducing conditions, the presence of free H_2S causes reduction of V to V(III), which may either be taken up by geoporphyrins or precipitated as a solid oxide (V_2O_3) or hydroxide ($V(OH)_3$) phase (Breit and Wanty 1991; Wanty and Goldhaber 1992). The two-step reduction process exhibited by V may result in the formation of separate V-bearing phases with differential solubilities under nonsulfidic anoxic versus euxinic conditions (Breit and Wanty 1991; Calvert and Pedersen 1993). Under anoxic conditions, Cr(VI) is reduced to Cr(III), forming aqua-hydroxyl or hydroxyl cations (e.g., $Cr(OH)_2^+$) that can be precipitated as insoluble $Cr(OH)_3$ or Cr_2O_3 at high pH (Elderfield 1970; Emerson et al. 1979; Drever 1997). At low pH, $Cr(OH)_2^+$ is thought to be readily complex with humic and fulvic acids and be adsorbed by Fe- and Mn-oxyhydroxides, which may provide transport vectors for increased Cr export to the sediment under anoxic conditions (Achterberg et al. 1997). Cr(III) uptake by authigenic Fe-sulfides is limited due to structural and electronic incompatibilities with pyrite crystals (Huerta-

Diaz and Morse 1992; Morse and Luther 1999). However, Pašava et al. (2021) reported elevated concentrations of Cr in synsedimentary pyrite formed under euxinic conditions from Ediacaran black shales at Liblín (TBU). In the euxinic facies, V resides predominantly in the "sulfidic" fraction (Algeo and Maynard 2004).

The mineralogy of V and Cr in black shales is rather complex. In modern marine environments (especially in anoxic non-sulfidic environments), V and Cr are commonly associated with organic matter (e.g., Francois 1988; Emerson and Huested 1991). Besides organometallic complexes, vanadium can be present in the form of sulfides, silicates, oxides and vanadates, depending on the transformation process (Yudovich, Ketris 1994). Chromium does not form an insoluble sulfide (Morse and Luther 1999) and is hosted mainly by organic and detrital phases, possibly with some accumulation as an independent Cr-oxyhydroxide phase (Algeo and Maynard 2004).

Here, we provide basic geochemical characteristics and a detailed ore-mineralogical study of the Neoproterozoic black shales from the Blovice Accretionary Complex (BAC), part of the Teplá–Barrandian Unit that were thermally affected by the intrusion of the Central Bohemian Pluton (Variscan age).

2. Geological setting

The studied section of black shales at Chynín is located in the Blovice Accretionary Complex (BAC), representing the predominant Cadomian basement of the Teplá–Barrandian Unit. The BAC formed during subduction of an oceanic plate beneath northern Gondwana during the Neoproterozoic–Cambrian (e.g., Žák et al. 2020 and references therein). The BAC consists of six linear belts, where three belts are dominated by coherent arc-derived and multiple recycled deep-marine siliciclastic successions (Belts I–III; Fig. 1), alternating with ocean-floor-bearing (ophiolitic) mélanges (Belts 1–3; Fig. 1; see Hajná et al. 2013, 2014 for more details) that contain tholeiitic as well as alkaline basaltic rocks representing members of Ocean Plate Stratigraphy (Ackerman et al. 2019a). Within the BAC, black shales are widespread, forming either (1) the so-called Lečice Member – a strongly silicified succession that intimately overlies the Davle Volcanic Complex (Ackerman et al. 2021) or (2) stratiform layers within siliciclastic successions (e.g., Kurzweill et al. 2015; Pašava et al. 2021). The latter type of black shales forms up to ~160–170 m thick horizons and has low TOC and low S (< 1 wt. %). These shales contain layers (up to 45 m thick) of metal-rich black shales with higher TOC-S.

The 250 m deep Chynín borehole (CHY-2) is located within the mélange-type Belt 1 of the BAC, and it was drilled within the exploration program of the Czechoslovak Uranium Enterprise in 1984, focused on evaluating the uranium potential of black shale formations in the Teplá–Barrandian Unit (TBU). The borehole CHY-2 encountered a volcano-sedimentary sequence made up of, from top to bottom:

– About 73 m thick package of tectonically affected grayish siltstone, locally with intercalations of black shale (up to 0.7 m thick) and pyrite along joints/fissures,
– About 36 m thick package of mostly brecciated metasilicites (cherts) with mostly centimeter-size slump balls of black shale with variable pyrite content,
– About 89 m thick package of fine-grained, dark gray to black, laminated and silicified black shales with abundant Fe sulfides (pyrite and pyrrhotite), containing about 6 m thick layer of light gray brecciated metasilicite (chert),
– About 51 m thick package of greenish gray strongly calcareous tuffites with abundant Fe-sulfides (dominantly pyrrhotite).

It should be noted that besides the close association of black shales with basic volcanogenic rocks and metasilicites, 1 : 50 000 scale geological mapping in this area resulted in the delineation of several bodies of hornfels along the contact zone with the Central Bohemian Pluton (CBP) (Map server of Czech Geological Survey). Cháb and Suk (1974) suggested that this region belongs to the Cadomian low-grade metamorphosed (prehnite-pumpellyite) zone, which was locally thermally affected by the intrusion of the CBP (Variscan age).

3. Methods and samples

Altogether eleven samples of black shales from the 250 m deep CHY-2 borehole were analyzed for major and selected trace elements, including the REE. The major element compositions were determined by wet-chemical methods techniques using the combination of atomic absorption spectroscopy (AAS), flame photometry and titration (see Dempírová et al. 2010) in the laboratory of the Czech Geological Survey. The precision of analyses was better than 5 rel. %, whereas the accuracy, which was monitored by the long-term reproducibility of selected reference materials (e.g., JGB-3), was better than 10 rel. % for all the analyzed oxides. Total organic carbon (TOC) and total sulfur of rock samples were determined using infra-red carbon and sulfur analyzer Eltra CS500 (Eltra, Neuss, Germany) and carbonate CO_2 on a Coulomat 7012 Strohlein instrument in the laboratory of the Czech Geological Survey.

Trace element contents were measured by ICP-MS using a Thermo iCAP-Q instrument at the Faculty of Science, Charles University, following the methods sum-

Tab. 1 Major and trace element concentrations in black shales from Chynín (TBU) (n = 11).

Sample	min	max	average	SD	median
SiO_2 wt.%	47.20	66.26	59.99	5.17	59.75
TiO_2	0.34	0.64	0.47	0.09	0.51
Al_2O_3	8.69	13.50	11.08	1.47	11.19
Fe_2O_3	0.02	3.13	0.62	0.93	0.13
FeO	3.63	18.28	9.09	3.99	7.45
MgO	1.55	3.85	2.27	0.74	1.93
MnO	0.04	0.19	0.08	0.05	0.06
CaO	0.47	3.57	1.00	0.89	0.62
Na_2O	0.85	2.83	1.41	0.65	1.14
K_2O	1.90	4.32	3.40	0.68	3.61
P_2O_5	0.08	0.17	0.12	0.03	0.12
F	0.03	0.08	0.05	0.02	0.06
CO_2	0.06	1.00	0.30	0.32	0.11
C(ost.)	2.26	4.63	3.69	0.78	3.67
S(tot.)	2.75	10.37	5.60	2.41	5.22
$H_2O(+)$	1.19	2.49	1.99	0.32	2.01
$H_2O(-)$	0.07	0.76	0.34	0.18	0.30
F(ekv)	0.01	0.03	0.02	0.01	0.03
S(ekv)	0.81	2.89	1.63	0.58	1.41
Total	99.14	100.56	99.85	0.49	99.92
V (ppm)	81	439	341	96	348
Cr	55	286	125	74	92
Co	8	52	22	11	18
Ni	36	254	136	56	129
Cu	51	307	186	65	194
Zn	68	572	361	166	378
Mo	10	116	49	25	47
Cd	0.1	11	6	3	6
Sb	1.0	7.0	3.5	1.5	3.3
La	25	40	29	4	28
Ce	48	82	59	12	51
Pr	6	9	7	1	7
Nd	25	37	29	4	28
Sm	5	8	6	1	6
Eu	1	2	1	bdl.	1
Gd	5	9	6	1	6
Tb	1	1	1	bdl.	1
Dy	4	9	6	1	5
Ho	1	2	1	bdl.	1
Er	2	6	4	1	4
Tm	bdl.	1	bdl.	bdl.	bdl.
Yb	2	5	3	1	3
Lu	bdl.	1	bdl.	bdl.	bdl.
Pb	9	32	22	7	21
Th	7	11	9	1	8
U	5	24	10	6	7
suma *REE*	129	202	152	22	142
TOC/P molar	167	161	181	146	180

SD – standard deviation; bdl. – analysis below the detection limit

marized in Strnad et al. (2005). The in-run precision was always better than 5 % (relative standard deviation) and the accuracy based on the analyses of SBC-1 and SGR-1b certified reference materials (USGS) was better than 12 % for all analyzed elements.

The polished sections were first studied using reflected light microscopy. Mineralogical analyses were completed using an FE-SEM Tescan Mira3 GMU fitted with an Oxford Instruments X-Max 80 (80 mm² active area) energy-dispersive spectrometer (EDS). In contrast, EBSD analyses were done using Oxford Instruments Symmetry (20 kV, 5 nA, software "Ox. Inst. AZtec", 8 belts for indexing, MAD ~0.1–0.5) at the Czech Geological Survey. Quant optimization was performed on a cobalt standard.

A set of synthetic elemental and mineral standards was used for the EDS analysis, and the analytical conditions were 15 kV accelerating voltage, 15 mm working distance (WD), 2 nA probe current, and 40 s counting time. Subsequently, selected mineral phases were analyzed by a CAMECA SX 100 electron microprobe at the Joint Laboratory of Electron Microscopy and Microanalysis of the Czech Geological Survey and Masaryk University in Brno. Quantitative analyses were performed using wavelength dispersive spectrometry with an accelerating voltage of 25 kV, beam current 20 nA, and beam diameter of 1 μm. Signals and standards used: VK_α (vanadinite), CrK_β (Cr), FeK_α (hematite), MnK_α (spessartine), TiK_α (TiO), AlK_α (sanidine), MgK_α (pyrope).

4. Results

4.1. Geochemistry of black shales

The main geochemical characteristics of black shales from the CHY-2 borehole are summarized in Tab. 1. The shales have on average 60 wt. % SiO_2 and show marked enrichment in TOC between 2.3 and 4.6 wt. % (average 3.7 wt. %) and sulfur (total sulfur contents vary from

2.7 to 10.4 wt. %, on average 5.6 wt. %); they belong to metal-rich black shales as defined by Pašava (2000). This is reflected in high levels of several metals (Zn up to 572 ppm, V up to 439 ppm, Cu up to 307 ppm, Ni up to 254 ppm, Cr up to 286 ppm, Mo up to 116 ppm, Co up to 52 ppm, Pb up to 32 ppm, and U up to 24 ppm).

4.2. Mineralogical characteristics

A typical black shale at Chynín is fine-grained organic-rich sediment with numerous quartz-rich layers. Its matrix comprises quartz, diopside, muscovite, biotite, graphite, K-feldspar, calcite, titanite and chlorite, and it contains accessory apatite, rutile, monazite, xenotime, and abundant iron sulfides. The mineral assemblage and the presence of parallel alignment of quartz, micas and chlorite resulting in a weak schistosity indicate that the black shales were subject to low-grade regional metamorphism.

4.2.1. Sulfides

The most common sulfides are pyrite and pyrrhotite, with less frequent chalcopyrite and sphalerite.

Pyrite I (syngenetic) occurs in the form of small framboids (up to 5 μm in size) dispersed in the rock matrix (Fig. 2a).

Pyrite II (recrystallized) forms larger (> 50 μm) and somewhat porous grains of cubic habit, representing recrystallized framboidal aggregates (Fig. 2b). Pyrite II grains commonly contain framboids of the original pyrite I and pyrrhotite. These framboids are separated from the sulfide matrix by a thin discontinuous layer of organic carbon.

Pyrite II is mostly homogeneously dispersed. Only locally, it forms sulfide layers up to 2 mm thick. Sulfide (dominated by pyrite) veinlets are both stratiform (Fig. 2a) and diagonal and are always rimmed by quartz (Fig. 2a).

Pyrrhotite forms coarse aggregates and replaces pyrite I (framboidal pyrite) and pyrite II (larger grains) (Fig. 2c). Newly formed pyrrhotite aggregates commonly show similar extinction for several grains, which is evidence for similarly oriented pyrrhotite grains structure even for separated grains, which originated during the transformation of pyrite into pyrrhotite (replacement of pyrite by pyrrhotite). Pyrrhotite formation was a response to the thermal effects on the host rock. Sulfide coarse aggregates always follow lamination.

Chalcopyrite and **sphalerite** are locally present in small grains intergrown with pyrite II and pyrrhotite. Sphalerite contains from 3.7 to 11.4 wt. % Fe, 0.5 to 1.2 wt. % Cd and rarely also Mn (up to 3.8 wt. %).

Molybdenite is even less common than Cu- and Zn-sulfides, and forms small flaky aggregates (up to 30 μm long) in the rock matrix or in Fe-sulfides. We also identified one 20 μm grain of **breihauptite** (NiSb) in association with **pentlandite** (($Fe_xNi_y)_{\Sigma 9}S_8$) in calcite matrix.

4.2.2. V–Cr–O phases

The anhedral grains of V–Cr–O phase reach up to 50 μm in size (exceptionally up to 0.1 mm) and occur exclusively in pyrrhotite, which they replace (never replacing pyrite and/or silicates, Fig. 2c). Replacement of pyrrhotite by the V–Cr–O phase begins at the contact with pyrrhotite grains and is selective, such that framboids may contain preserved pyrrhotite cores (Fig. 2d) whose similar extinction with surrounding pyrrhotite provides evidence for the similar orientation of the crystal lattice. This (V–Cr–O) mineral phase is free of any inclusions and its grains are preferentially bound to layers composed of abundant grainy aggregates of Fe-sulfides. Based on EBSD data, it has a corundum-type structure. Its chemical composition (Tab. 2) indicates solid solution between predominant karelianite (V_2O_3) and subordinate eskolaite (Cr_2O_3) end-member, with a low content of the hematite end-member (Fe_2O_3). Lower totals (analyses 3, 5 and 6 in Tab. 2) could reflect alteration of grains, which was, however, not observed under BSE. Complete mixing in the system V_2O_3–Cr_2O_3 was described by Reid et al. (1972), who also noted extensive solid-solution in the systems V_2O_3–Al_2O_3 and V_2O_3–Fe_2O_3.

4.2.3. Ti–V–Fe–Cr phases

The Ti–V–Fe–Cr mineral phases were found in association with sulfides and the karelianite–eskolaite, where they form inhomogeneous anhedral grains (Fig 2e). The mineral grains are composed of lamellae formed by different phases; their chemical composition is given in Tab. 3. These phases are vanadium rutile (V-rutile), schreyerite ($V_2Ti_3O_9$) and a phase with the theoretical composition of $V_4Ti_3O_{12}$, not yet known in the mineral system. EBSD confirmed vanadium rutile (2 analyses) and schreyerite. Vanadium rutile contains 2.49 and 5.62 wt. % V, respectively, and its calculated formulae correspond to $Ti_{0.94}V_{0.05}Fe_{0.01}O_2$ and $Ti_{0.87}V_{0.12}Fe_{0.01}O_2$, respectively (Tab. 3).

Schreyerite, first described by Medenbach and Schmetzer (1978), dominantly forms polysynthetic twin lamellae in V-rutile formed by exsolution. Its chemical compositions and empirical formulae are given in Tab. 3. The mineral phase with the idealized formula $V_4Ti_3O_{12}$ found at Chynín has not been synthesized yet (Brach et al. 1977; Döbelin et al. 2006). It can represent either a
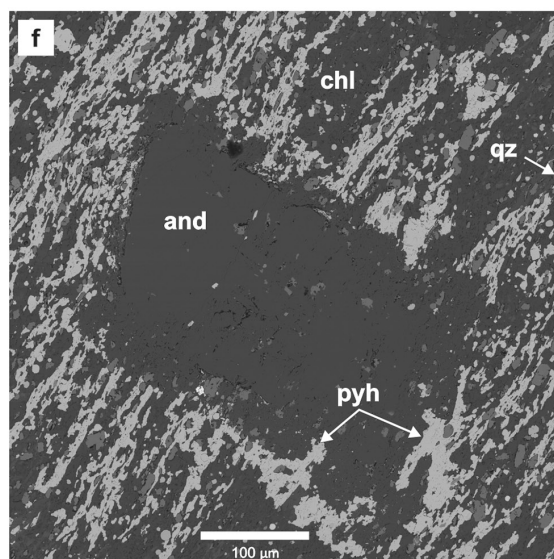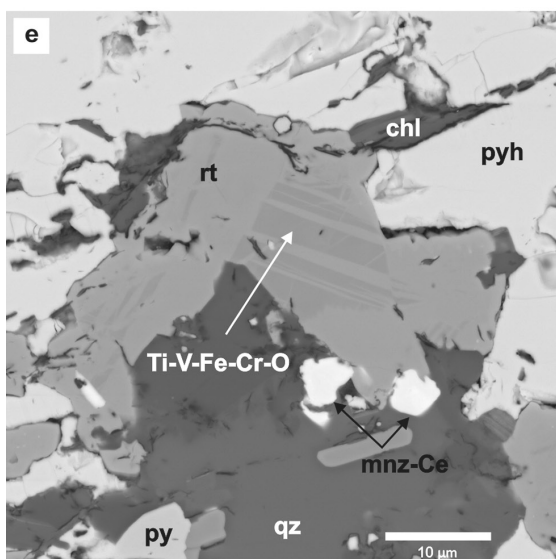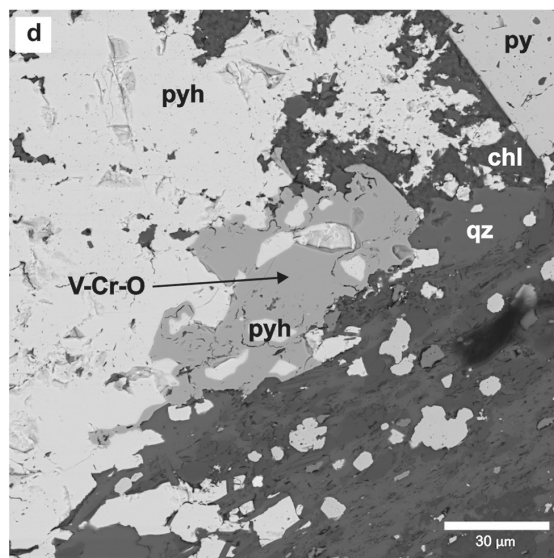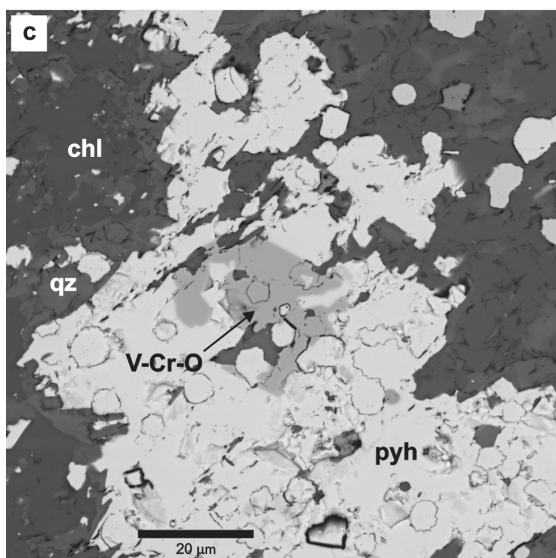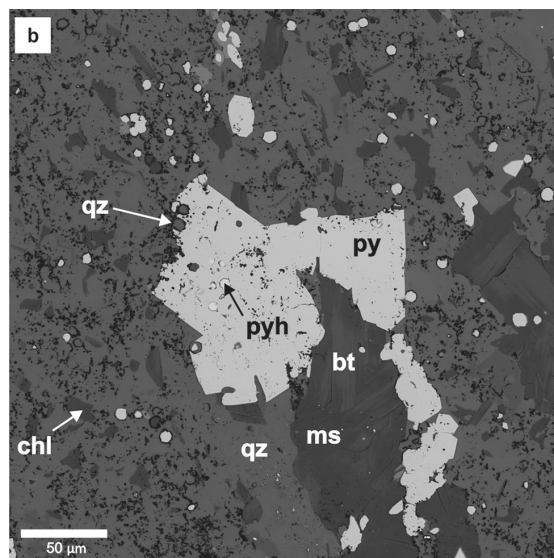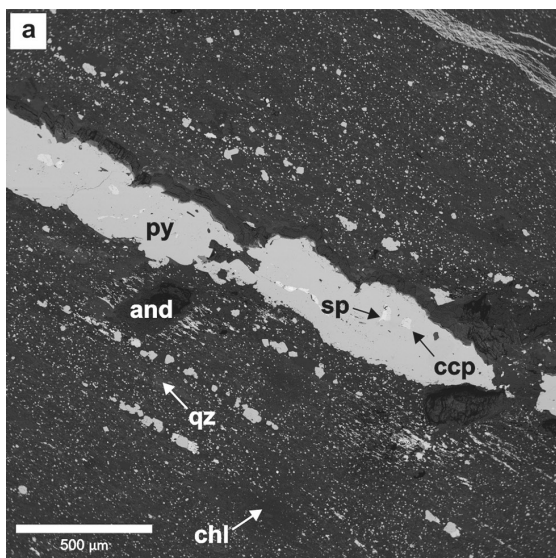
Tab. 2 EPMA chemical composition of V–Cr oxide phases in black shales from Chynín (TBU).

wt. %								*apfu*					
V_2O_3	Cr_2O_3	Fe_2O_3	Mn_2O_3	TiO_2	Al_2O_3	MgO	Total	#	V	Cr	Fe	Mn	Al
76.69	20.29	1.40	bdl.	bdl.	bdl.	bdl.	98.39	2	1.56	0.41	0.03	bdl.	bdl.
74.53	22.31	1.24	0.07	bdl.	bdl.	bdl.	98.16	4	1.52	0.45	0.02	bdl.	bdl.
86.28	12.93	0.93	bdl.	bdl.	bdl.	bdl.	100.15	7	1.73	0.26	0.02	bdl.	bdl.
90.06	9.41	0.59	bdl.	bdl.	bdl.	0.03	100.09	8	1.80	0.19	0.01	bdl.	bdl.
89.94	9.50	0.70	bdl.	bdl.	bdl.	bdl.	100.14	9	1.80	0.19	0.01	bdl.	bdl.
90.32	9.47	0.58	bdl.	bdl.	bdl.	bdl.	100.37	10	1.80	0.19	0.01	bdl.	bdl.
82.93	16.26	1.09	bdl.	bdl.	bdl.	bdl.	100.28	11	1.66	0.32	0.02	bdl.	bdl.
89.05	10.56	0.82	bdl.	bdl.	0.08	bdl.	100.51	12	1.77	0.21	0.02	bdl.	bdl.
88.52	10.99	0.86	bdl.	bdl.	bdl.	bdl.	100.36	13	1.77	0.22	0.02	bdl.	bdl.
85.40	13.37	1.17	0.07	bdl.	bdl.	bdl.	100.00	14	1.71	0.26	0.02	bdl.	bdl.
82.95	15.13	0.99	bdl.	bdl.	bdl.	bdl.	99.08	15	1.68	0.30	0.02	bdl.	bdl.
82.58	16.44	1.36	0.07	bdl.	bdl.	bdl.	100.45	16	1.65	0.32	0.03	bdl.	bdl.
81.82	16.84	1.31	0.06	bdl.	0.06	bdl.	100.10	17	1.64	0.33	0.02	bdl.	bdl.
75.50	23.23	1.27	bdl.	bdl.	bdl.	bdl.	100.00	18	1.52	0.46	0.02	bdl.	bdl.
78.94	19.74	1.22	bdl.	bdl.	bdl.	bdl.	99.89	19	1.59	0.39	0.02	bdl.	bdl.
69.24	29.74	1.61	0.11	bdl.	bdl.	bdl.	100.71	20	1.38	0.59	0.03	bdl.	bdl.
67.99	31.57	1.39	0.10	bdl.	0.05	bdl.	101.10	21	1.35	0.62	0.03	bdl.	bdl.
71.61	27.61	1.12	0.09	bdl.	0.16	bdl.	100.59	22	1.43	0.54	0.02	bdl.	bdl.
71.46	27.05	1.24	0.08	bdl.	0.28	bdl.	100.11	23	1.43	0.53	0.02	bdl.	0.01
88.15	5.28	6.36	0.08	0.37	0.13	0.04	100.41	24	1.76	0.10	0.12	bdl.	bdl.
58.14	6.07	30.65	4.48	bdl.	0.74	0.35	100.45	26	1.18	0.12	0.59	0.09	0.02
47.27	17.61	19.12	15.07	bdl.	0.14	0.17	99.38	27	0.97	0.36	0.37	0.29	bdl.
52.68	13.40	20.28	14.88	bdl.	0.18	0.14	101.57	28	1.06	0.27	0.38	0.28	0.01
89.04	4.63	5.63	0.09	0.17	0.11	0.03	99.69	29	1.80	0.09	0.11	bdl.	bdl.
89.80	4.19	5.19	0.08	0.12	0.08	0.04	99.50	30	1.81	0.08	0.10	bdl.	bdl.

Bdl. – analysis was below the limit of the detection; negative contents: Ti, Mg, Zn, S.

metastable phase or a structural mixture represented by a combination of structural chains of berdesinskiite type (V_2TiO_5 type) and chains of Ti_2O_4 type (high-pressure phase of TiO_2 with α-PbO_2 structure). The two chain types, in the 1:1 ratio, form the structure of schreyerite.

⇐

Fig. 2 SEM/BSE photomicrographs of the mineral association in metal-rich black shales from Chynín. **a** – Abundant framboidal pyrite I (replaced mainly by pyrrhotite) dispersed in TOC-rich matrix with quartz-sulfide (dominated by pyrite) stratiform veinlets. **b** – Larger cubic grains of recrystallized framboidal pyrite (pyrite II) and pyrrhotite replacing original framboids of pyrite. **c** – Pyrrhotite forms coarse aggregates and replaces pyrite I (framboidal pyrite) and pyrite II (larger grains) with anhedral grains of V–Cr–O phases which most effectively replace pyrrhotite. **d** – Replacement of pyrrhotite by V–Cr–O phases initiates at the rim of pyrrhotite grains and is selective, such that framboids can contain preserved pyrrhotite cores. **e** –Anhedral grains of Ti–V–O mineral phases (V-rutile, schreyerite and two other phases, not yet known in the mineral system) associated with pyrrhotite. **f** – Large euhedral grain of andalusite with small number of inclusions (e.g., apatite and monazite-(Ce)). Growth of andalusite was also accompanied by dissolution of sulfide framboids and re-precipitation of pyrrhotite immediately front of growing crystal, forming pyrrhotite grainy aggregates that follow host rock lamination.
py - pyrite, ccp - chalcopyrite, sp – sphalerite, pyh – pyrrhotite, qz – quartz, V–Cr–O – karelianite-eskolaite, Ti–V–Fe–Cr–O – V-rutile, schreyerite and a phase, not yet known in the mineral system, mnz-Ce – monazite-Ce, and – andalusite.

4.2.4. Other minerals

The groundmass of the black shale is formed primarily of quartz, andalusite, diopside, muscovite, calcite, titanite, chlorite, apatite, rutile, K-feldspar, monazite (Ce), and xenotime. Except for andalusite and calcite, all other rock forming-minerals form anhedral isolated grains (up to 20 μm in size). Only biotite, chlorite and muscovite (locally also diopside) are subhedral. Interestingly, chlorite, biotite and diopside have very low or zero Fe content. All rutile grains have elevated V contents (2.3 to 3.8 wt. %, Tab. 3).

A single grain of xenotime was found, far from the ideal formula of YPO_4 (containing more than 4 wt. % REE only, analysis not shown in tables). Thorium, U and Y concentrations in monazite-Ce from Chynín are below the detection limit.

Andalusite (verified by EBSD) forms euhedral (rhomboid) relatively large (up to 0.3 mm) porphyroblasts, overgrowing the fabric of the shales. These grains contain a small number of inclusions (e.g., apatite and monazite-Ce; Fig. 2f). The presence of large porphyroblasts of andalusite overgrowing the rock fabrics reflects an effect of subsequent contact metamorphism.

Tab. 3 EPMA chemical composition of Ti–V oxide phases in black shales from Chynín (TBU).

	1	25	31	32	33	34
Fe_2O_3	1.75	3.99	1.52	1.89	0.71	1.05
Mn_2O_3	bdl.	bdl.	bdl.	0.06	bdl.	bdl.
TiO_2	55.43	44.67	60.05	57.95	95.78	89.75
Al_2O_3	0.26	0.15	0.18	0.19	bdl.	bdl.
MgO	0.02	0.02	0.02	0.02	bdl.	bdl.
V_2O_3	39.83	50.71	39.17	39.69	4.44	10.03
Cr_2O_3	2.34	1.11	0.65	bdl.	bdl.	bdl.
Total	99.62	100.65	101.59	99.80	100.94	100.83

#	Phase	Empirical formula
1	schreyerite	$(V_{2.11}Cr_{0.12}Fe_{0.10}Al_{0.02})Ti_{2.76}O_9$
25	$V_4Ti_3O_{12}$	$(V_{3.67}Cr_{0.12}Fe_{0.30}Al_{0.02})Ti_{3.03}O_{12}$
31	schreyerite	$(V_{2.02}Fe_{0.08}Cr_{0.03}Al_{0.01})Ti_{2.91}O_9$
32	schreyerite	$(V_{2.09}Fe_{0.10}Al_{0.01})Ti_{2.87}O_9$
33	rutile	$Ti_{0.96}V_{0.05}Fe_{0.01}O_2$
34	rutile	$Ti_{0.91}V_{0.11}Fe_{0.01}O_2$

Bdl. – analysis was below the limit of the detection.

5. Discussion

5.1. Depositional environment of black shales and diagenetic processes

The chondrite-normalized REE patterns of the black shales are characteristic of crustal rocks, being variably LREE-enriched (La_N/Yb_N = 4.8–13) with pronounced negative Eu anomalies (Eu/Eu* = 0.6–0.8), indicating a predominantly terrigenous source of the REE. Collectively, high TOC values, TOC/P molar
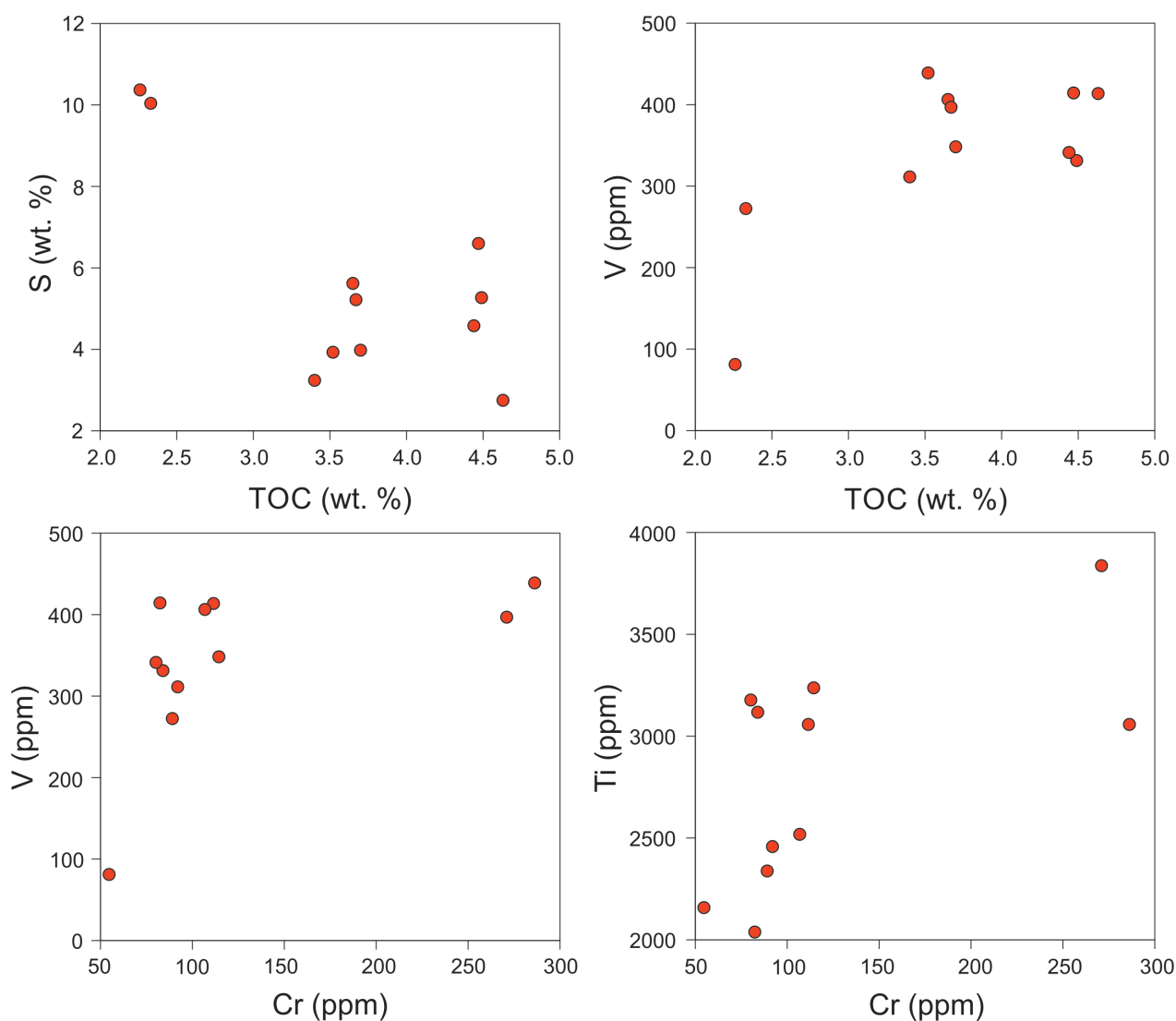
Fig. 3 Plots of TOC *vs.* S and V and between Cr and Ti and V in the thermally affected black shales from Chynín, documenting significant redistribution of metals. Significant positive correlations were found only between TOC and V (r = 0.69) and between Ti and Cr (r = 0.6).

ratios higher than 100 (average 181), and high Mo and U contents (up to 116 and 24 ppm, respectively) suggest that Chynín black shales were deposited under highly reducing conditions (e.g., Algeo and Tribovillard 2009; Algeo and Li 2020). On the other hand, the absence of well-defined correlations between TOC contents and redox-sensitive metals (e.g., V, U, Cr, Ni, Mo), together with their generally decreasing contents with increasing S concentrations, indicate significant late-stage metal and sulfur remobilization. Yet, V and Mo are most likely hosted by authigenic organic matter, while Cr and Ti seem to be bound to detrital components (Fig. 3).

The low Th, U and Y contents in monazite indicate its formation during the diagenetic process (Čopjaková et al. 2011), which agrees with conclusions of Scharm and Scharmová (1995) regarding the formation of monazite in cherts from the Kokšín locality.

5.2. Implications of geochemical data for the formation of V-rich phases at Chynín locality

Geochemical evidence (increased TOC, S, Mo and U values) in our black shales supports highly reducing conditions at Chynín. High contents of reactive sulfur and preferential bonding with Fe are documented by a significant positive correlation between S and FeO ($r = 0.9$) and the absence of Fe-silicate phases in the rock matrix (chlorite, biotite and diopside are purely Mg-rich phases). Positive correlations between TOC and V ($r = 0.69$), Cr and Ni ($r = 0.89$) and Cr and TiO_2 ($r = 0.88$) at Chynín suggest that authigenic organic matter was a source of V (as, e.g., documented by Emerson and Huested, 1991 on an example of modern marine sediments). In contrast, Cr and Ti were likely derived from detrital sources, such as, e.g., reported by Algeo and Maynard (2004) reported from Pennsylvanian black shales (Kansas, USA).

5.3. Thermal effect and desulfurization of pyrite

The mineral parageneses in the black shales at Chynín, involving metamorphic phases such as chlorite, biotite, muscovite and graphite, reflect a regional metamorphic overprint of these rocks. Andalusite with perfect crystal shape overgrows the foliation and thus must have formed after regional metamorphism and deformation of the black shale. The geological context suggests that andalusite formation reflects contact metamorphism due to the emplacement of the Central Bohemian Pluton. The origin of andalusite is limited to the temperature interval 200–750 °C and pressures up to 4 kbar (Howie 2005). We suggest that its growth at elevated temperature was accompanied by dissolution of sulfide framboids and re-

precipitation of pyrrhotite in the immediate front of the growing crystal, forming pyrrhotite grainy aggregates following the host rock fabric.

At laboratory conditions in a vacuum, desulfurization of pyrite begins above 500 °C and the process of pyrrhotite formation (with the release of S_2) terminates at 800 °C (Xu et al. 2019). However, such a dry process is not very likely at Chynín as we see, that parts of framboids were replaced by quartz. The release of V, Cr and Ti from the host-rock at Chynín was accompanied by the formation of V–Cr–O and V–Ti–Fe–Cr–O phases.

5.4. Examples of formation of V-Cr-Ti rich phases worldwide

Schreyerite and minerals of the karelianite-eskolaite group were described from several localities worldwide in rocks with anomalous V (Cr, Ti) concentrations, which were metamorphosed under amphibolite-facies conditions, and which are associated with Fe, base metal sulfide, U–V, and Au deposits (Zakrzewski et al. 1982; Höller and Stumpfl 1995; Höller and Gandhi 1997; Döbelin et al. 2006). Schreyerite and minerals of the karelianite-eskolaite group are intimately associated with pyrrhotite, similar to Chynín, where black shales have elevated base metal, U and V contents. For example, Zakrzewski et al. (1982) interpreted the origin of schreyerite at the Sätra pyrite deposit (Bergslagen district, Sweden) to be the result of pyrrhotite formation during remobilization of disseminated Fe-sulfide mineralization. Based on the presence of andalusite–cordierite–quartz–muscovite–microcline assemblage, they estimated conditions of remobilization at 2–3 kbar and T ~ 550 °C. Canet et al. (2003) documented that the contact metamorphism of lower Silurian V- and Cr-rich sulfidic black shale produced metapelitic hornfels with V-rich aluminosilicates and V–Cr oxides accompanied by mainly pyrrhotite and minor chalcopyrite. The occurrence of V oxides in apparent equilibrium with V-rich silicates suggests a solubility limit for V and Cr in these aluminosilicates at the conditions of thermal metamorphism. On the other hand, metamorphism of anorthite- and V, Cr-rich sedimentary rocks produces V- and Cr-rich silicates, such as goldmanite, V-rich amphiboles, V-rich titanite and V-rich allanite (Canet et al. 2003). Similar to the Outokumpu deposit (Finland) and the Nairne deposit (Australia), these V(Cr,Ti) phases must have formed in a strongly reducing environment with extremely high sulfur fugacity ($f S_2$) (Long et al. 1963; Graham 1978). The small framboid sizes (< 5 μm) point to their origin in a strongly reducing (euxinic) environment (Rickard 2019).

Höller and Stumpfl (1995) suggested that at the Rampura Agucha base metal deposit (India), clay minerals, chlorite and organic matter served as a source (precursor)

of V and Cr. They proposed that during prograde metamorphism and formation of silicates and graphite, V and Cr were liberated and captured in V- and Cr-rich rutile. Decreasing P–T conditions resulted in the exsolution of schreyerite lamellae.

5.5. V–Cr–Ti association in Si-rich rocks of the Bohemian Massif

Scharm and Scharmová (1995) studied Neoproterozoic silexite (silicite with stromatolitic texture) at Kokšín near Mítov (ca. 10 km NW of Chynín) and identified a Ti–V–Cr oxide phase. It likely was one of our newly reported mineral phases despite different host lithologies (metal-rich black shales at Chynín and silicite at Kokšín). Houzar and Cempírek (2011) reported a new occurrence of schreyerite in the upper amphibolite facies graphite quartzite near Bítovánky, in the south-eastern part of the Moldanubian zone of the Bohemian Massif. Schreyerite is intergrown with V-rich rutile (0.044–0.058 V *apfu*) and occurs as isolated microscopic grains in the mineral assemblage: quartz + graphite + V-rich muscovite + V-rich dravite (lacking sulfides). Mrázek (1984, 1986) described anomalous Cr and V concentrations in Neoproterozoic silicites and interpreted them to result from the hydrothermal enrichment. Similarly, high V and Cr values (190–931 ppm) have been recently reported from Neoproterozoic silicites with stromatolitic texture (cherts) in the Brdy area by Stárková et al. (2018), who relate them to the combined effects of volcanogenic-hydrothermal and microbial activities. Hajná et al. (2019) reported 195 ppm V and 166 ppm Cr from layered-texture chert at Pelechovka (Belt I, TBU). Anomalous vanadium (average 691ppm, max. 2100 ppm, *n* = 47) that correlate well with TOC and Cr concentrations (average 190 ppm, max. 1200 ppm, *n* = 47) in Neoproterozoic metal-rich black shales of the TBU was reported by Pašava (2000). The presence of similar geochemical anomalies (V, Cr, (Ti)) in Neoproterozoic metal-rich black shales, their contact metamorphosed equivalents and (meta)silicites (cherts) in TBU most likely indicate a similar source of these elements. However, the different principal carriers in these lithologies reflect the specific conditions of their accumulation. In black shales, V is dominantly associated with TOC (organic matter) and Cr is usually derived from terrigenous material or can also be bound to organic matter or Fe sulfides (Ackerman et al. 2019b, 2021; Pašava 2000; Pašava et al. 2021; Bian et al. 2021). On the other hand, the absence of well-defined correlations between TOC contents and redox-sensitive metals (e.g., V, Cr, U, Ni, Mo) combined with their generally decreasing contents with increasing S concentrations in thermally affected black shales at Chynín indicate significant late-stage metal and sulfur remobilization. During this process, the discrete phases of V–Cr–O and V–Ti–O were formed. In Neoproterozoic silicites (cherts) of the TBU, V is usually bound to Fe-oxides (Stárková et al. 2018) or V-mica (roscoelite containing up to 5 wt. % Cr) and crandallite (with up to 6% V and Cr) (Gabriel 1991). Johan et al. (1995) described V and Cr in Mg-rich illite and/or gorceixite and florencite and also Cr-muscovite in stromatolitic silicites at Kokšín. The presence of goldmanite was reported by Litochleb et al. (1985) from black metasilicite of the U–V Struhadlo deposit (TBU).

6. Conclusions

Based on the study of black shales associated with metasilicites, metabasalts and basic tuffs and regionally accompanied by hornfels at Chynín (TBU), we show that:

1. Geochemical characteristics including high TOC values, TOC/P molar ratios > 100 and high Mo and U contents suggest deposition of metal-rich black shales at Chynín in a strongly reducing environment. This is supported by the presence of abundant diagenetic framboidal pyrite (pyrite I).

2. The mineral paragenesis of the black shales (including the presence of abundant andalusite) and their location in the proximity of the Central Bohemian Pluton indicate that these facies were regionally metamorphosed and thermally overprinted. This is also supported by abundant pyrrhotite, which formed because of selective desulfurization of pyrite I and II. Locally, this process was also accompanied by replacing pyrrhotite with V–Cr–O and Ti–V–O phases.

3. Similar elemental association of V, Cr, Ti in Neoproterozoic metal-rich black shales, their thermally overprinted equivalents and (meta)silicites (cherts) in the TBU and their different principal carriers in these lithologies most likely reflect similar sources of these elements and specific conditions of their accumulation.

References

ACHTERBERG EP, VAN DEN BERG CMG, BOUSSEMART M, DAVISON W (1997) Speciation and cycling of trace metals in Esthwaite water: a productive English lake with seasonal deep-water anoxia. Geochim Cosmochim Acta 61: 5233– 5253

ACKERMAN L, HAJNÁ J, ŽÁK J, ERBAN V, SLÁMA J, POLÁK L, KACHLÍK V, STRNAD L, TRUBAČ J (2019a) Architecture and composition of ocean floor subducted beneath northern Gondwana during Neoproterozoic to Cambrian: A palinspastic reconstruction based on Ocean Plate Stratigraphy (OPS). Gondwana Res 76: 77–97

ACKERMAN L, PAŠAVA J, ŠÍPKOVÁ A, MARTÍNKOVÁ E, HALUZOVÁ E, RODOVSKÁ Z, CHRASTNÝ V (2019b) Copper, zinc, chromium and osmium isotopic compositions of the Teplá–Barrandian unit black shales and implications for the composition and oxygenation of the Neoproterozoic–Cambrian ocean. Chem Geol 521: 59–75

ACKERMAN L, PAŠAVA J, ŽÁK J, ŽÁK K, KACHLÍK V, ŠEBEK O, TRUBAČ J, SVOJTKA M, VESELOVSKÝ F, STRNAD L, SANTOLÍK V (2021) Arc-related black shales as sedimentary archives of sea-level fluctuations and plate tectonics during the late Neoproterozoic: An example from the Bohemian Massif. Mar Pet Geol 123: 104713

ALGEO TJ, MAYNARD JB (2004) Trace-element behavior and redox facies in core shales of Upper Pennsylvanian Kansas-type cyclothems. Chem Geol 206: 289–318

ALGEO TJ, TRIBOVILLARD N (2009) Environmental analysis of paleoceanographic systems based on molybdenum–uranium covariation. Chem Geol 268: 211–225

ALGEO TJ, LI C (2020) Redox classification and calibration of redox thresholds in sedimentary systems. Geochim Cosmochim Acta 287: 8–26

ANDERSSON A, DAHLMAN B, GEE DE, SNALL S (1985) The Scandinavian Alum shales, Serie Ca, No. 56, Sveriges Geologiska Undersökning

BIAN L, SCHOVSBO NH, CHAPPAZ A, ZHENG X, NIELSEN AT, ULRICH T, WANG X, DAI S, GALLOWAY JM, MAŁACHOWSKA A, XU X, SANEI H (2021) Molybdenum-uranium-vanadium geochemistry in the lower Paleozoic Alum Shale of Scandinavia: Implications for vanadium exploration. Int J Coal Geol 239: 103730

BRACH B, GREY IE, LI C (1977) Phase Equilibria in the System V_2O_3–Ti_2O_3–TiO_2 at 1473 °K. J Solid State Chem 20: 29–41

BREIT GN, WANTY RB (1991) Vanadium accumulation in carbonaceous rocks: a review of geochemical controls during deposition and diagenesis. Chem Geol 91: 83–97

CALVERT SE, PEDERSEN TF (1993) Geochemistry of Recent oxic and anoxic marine sediments: implications for the geological record. Mar Geol 113: 67–88

CANET C, ALFONSO P, MELGAREJO JC, JORGE S (2003) V-rich minerals in contact-metamorphosed Silurian SEDEX deposits in the Poblet area, southwestern Catalonia, Spain. Canad Mineral 41: 561–579

CHÁB J, SUK M (1974) Regional metamophosis in Czech and Moravian area, pp 1–156. Ústřední ústav geologický, Praha (in Czech)

CHEN N, YANG X, LIU D, XIAO X, FAN D, WANG L (1990) Lower Cambrian black rock series and associated stratiform deposits in southern China. Chin J Geochem 8: 244–255

COVENEY RM JR (2000) Metalliferous black shales and the role of organic matter with examples from China, Poland and the United States. In: Giordano TH, Kettler RM, Wood SA (eds) Ore Genesis and Exploration: The Roles of Organic Matter. Rev Econ Geol 9: 251–280

COVENEY RM, CHEN N (1991) Ni-Mo-PGE-Au-rich ores in Chinese black shales and speculations on possible analogues in the United States. Miner Depos 26: 83–88

COVENEY RM, GLASCOCK A (1989) A review of the origins of metal-rich Pennsylvanian black shales, central U.S.A., with an inferred role for basinal brines. Appl Geochem 4: 347–367

COVENEY RM JR, PAŠAVA J (2004) Diverse connections between ores and organic matter. Ore Geol Rev 24:1–5

COVENEY RM, LEVENTHAL JS, GLASCOCK MD, HATCH JR (1987) Origins of metals and organic matter in the Mecca Quarry Shale Member and stratigraphically equivalent beds across the Midwest. Econ Geol 82(4): 915–933

ČOPJAKOVÁ R, NOVÁK M, FRANCŮ E (2011) Formation of authigenic monazite-(Nd) from Upper Carboniferous graywackes of the Drahany Upland: Roles of the chemical composition of host rock and burial temperature. Lithos 127: 373–385

DEMPÍROVÁ L, ŠIKL J, KAŠIČKOVÁ R, ZOULKOVÁ V, KŘÍBEK B (2010) The evaluation of precision and relative error of the main components of silicate analyses in Central Laboratory of the Czech Geological Survey. Geoscience Research Reports in 2009 (27): 326–330

DÖBELIN N, REZNITSKI L Z, SKLYAROV EV, ARMBRUSTER T, MEDENBACH O (2006) Schreyerite, $V_2Ti_3O_9$: New occurence and crystal structure. Amer Miner 91: 196–202

DREVER JI (1997) The Geochemistry of Natural Waters, 3rd ed. Prentice-Hall, Upper Saddle River, NJ, pp 1–436

ELDERFIELD H (1970) Chromium speciation in sea water. Earth Planet Sci Lett 9: 10–16

EMERSON SR, HUESTED S (1991) Ocean anoxia and the concentrations of molybdenum and vanadium in seawater. Mar Chem 34: 177–196

EMERSON SR, CRANSTON RE, LISS PS (1979) Redox species in a reducing fjord: equilibrium and kinetic considerations. Deep-Sea Res 26A: 859–878

FAN D (1983) Polyelements in the Lower Cambrian black shale series in southern China. In: AUGUSTITHIS SS (ed) The Significance of Trace Metals in Solving Petrogenetic Problems and Controversies. Theophrastus Publications S.A., Athens, pp 447–474

Francois R (1988) A study on the regulation of the concentrations of some trace metals (Rb, Sr, Zn, Pb, Cu, V, Cr, Ni, Mn and Mo) in Saanich Inlet sediments, British Columbia, Canada. Mar Geol 83: 285–308

Gabriel Z (1991) Upper Proterozoic chert hosted Au-Ni-V-Cr-Ba mineralization. In: Pagel M, Leroy JL (eds) Source, Transport and Deposition of Metals. (Proceedings of the 25 Years SGA Anniversary Meeting, Nancy 1991, A.A.Balkema, Rotterdam), 41–43

Graham J (1978) Manganochromite, palladium antimonide, and some unusual mineral associations at the Nairne pyrite deposit, South Australia. Amer Miner 63: 1166–74

Grauch RI, Huyck HLO (1990) Metalliferous Black Shales and Related Ore Deposits – Proceedings, 1989 United States Working Group Meeting, International Geological Correlation Program Project 254. U.S. Geological Survey Circular 1058, pp 1–85

Hajná J, Žák J, Kachlík V (2014) Growth of accretionary wedges and pulsed ophiolitic mélange formation by successive subduction of trench-parallel volcanic elevations. Terra Nova 26: 322–329

Hajná J, Žák J, Kachlík V, Dörr W, Gerdes A (2013) Neoproterozoic to early Cambrian Franciscan-type mélanges in the Teplá–Barrandian unit, Bohemian Massif: Evidence of modern-style accretionary processes along the Cadomian active margin of Gondwana? Precambrian Res 224: 653–670

Hajná J, Žák J, Ackerman L, Svojtka M, Pašava J (2019) A giant late Precambrian chert-bearing olistostrome discovered in the Bohemian Massif: a record of Oceanic Plate Stratigraphy (OPS) disrupted by mass-wasting along an outer trench slope. Gondwana Res 74: 173–188

Höller W, Gandhi SM (1997) Origine of tourmaline and oxide minerals from the metamorphosed Rampura Agucha Zn-Pb-(Ag) deposit, Rajasthan, India. Mineral Petrol 60: 99–119

Höller W, Stumpfl EF (1995) Cr–V oxides from the Rampura Agucha Pb–Zn–(Ag) deposit, Rajasthan, India. Canad Mineral 33: 745–752

Houzar S, Cempírek J (2011) Accesory schreyerite in vanadium-rich graphite quartzite at Bítovánky (Moldanubicum, western Moravia). Acta Mus Morav, Sci geol 96, 2: 35–43 (in Czech with English summary)

Howie RA (2005) Minerals/Other Silicates. In: Sellery RC, Cocks LRM, Plimer IR (eds) Encyclopedia of geology. Elsevier, Amsterdam, pp 561–569

Huerta-Diaz MG, Morse JW (1992) Pyritization of trace metals in anoxic marine sediments. Geochim Cosmochim Acta 56: 2681–2702

Jeong GY (2006) Mineralogy and geochemistry of metalliferous black slates in the Okcheon metamorphic belt, Korea: a metamorphic analogue of black shales in the South China block. Miner Depos 41: 469–481

Johan Z, Johan V, Scharm B, Pouba Z (1995) Minéralogie et géochimie des terres rares et du chrome dans les cherts protérozoiques de Kokšín, République tcheque. C R Acad Sci Paris, t. 321, II a, 1127–1138

Kurzweil F, Drost K, Pašava J, Wille M, Taubald H, Schoeckle D, Schoenberg R (2015) Coupled sulfur, iron and molybdenum isotope data from black shales of the Teplá–Barrandian unit argue against deep ocean oxygenation during the Ediacaran. Geochim Cosmochim Acta 171: 121–142

Lehmann B, Frei R, Xu L, Mao J (2016) Early Cambrian black shale-hosted Mo–Ni and V mineralization on the rifted margin of the Yangtze Platform, China: Reconnaissance chromium isotope data and a refined metallogenic model. Econ Geol 111: 89–103

Leventhal J (1993) Metals in black shales. In: Engel MH, Macko SA (eds) Organic Geochemistry: Principles and Applications. Plenum Press, New York, pp 581–607

Litochleb J, Novická Z, Burda J (1985) Vanadian garnets in Proterozoic metasilicites from Struhadlo near Klatovy. Čas Nár muz, Ř Přírod 151: 31–34 (in Czech)

Long J, Vuorelainen Y, Kouvo O (1963) Karelianite, a new vanadium mineral. Amer Miner 48: 33–41

Loukola-Ruskeeniemi K (1991) Geochemical evidence for the hydrothermal origin of sulphur, base metals and gold in Proterozoic metamorphosed black shales, Kainuu and Outokumpu areas, Finland. Mineral Depos 26: 152–164

Loukola-Ruskeeniemi K (1999) Origin of black shales and serpentinite-associated Cu–Zn–Co ores at Outokumpu in Finland. Econ Geol 94: 1007–1028

Loukola-Ruskeeniemi K, Lahtinen H (2012) Multiphase evolution in the black-shale-hosted Ni–Cu–Zn–Co deposit at Talvivaara, Finland. Ore Geol Rev (2012), 85–99

Love JD (1967) Anatomy of the Western Phosphate Field. Fifteenth Annual Field Conference, A Guide to the Geologic Occurrence, Exploration Methods, Mining Engineering, Recovery Technology, pp 115–118

Map server of Czech Geological Survey, http://www.geology.cz/app/ciselniky/lokalizace/show_map.php?mapa=g50&y=801500&x=1094000&r=3500&s=1&legselect=0

Medenbach O, Schmetzer K (1978) Schreyerite, $V_2Ti_3O_9$, a new mineral. Amer Miner 63: 182–186

Morse JW, Luther GW (1999) Chemical influences on trace metal–sulfide interactions in anoxic sediments. Geochim Cosmochim Acta 63: 3373–3378

Mrázek P (1984) Geochemistry of rock of Barrandien. Acta Univ Carol, Geol 30: 251–252 (in Czech)

Mrázek P (1986) Metalogenetic processes in western Czech upper Proterozoicum. Věst Ústř Úst Geol 61, 4: 233–241 (in Czech)

Oszczepalski S (1989) Kupferschiefer in southwestern Poland: Sedimentary environments, metal zoning, and ore controls. In: Boyle RW, Brown AC, Jefferson GF, Jowett EC, Kirkham RV (eds) Sediment-hosted

Stratiform Copper Deposits. Geol Assoc Can, Spec Pap 36: 57–600

Pašava J (1993) Anoxic sediments – an important source for PGE; an overview. Ore Geol Rev 8: 425–445

Pašava J (2000) Normal versus metal-rich black shales in the Barrandian Neoproterozoic of the Tepla–Barrandian Unit: A summary with new data. Věst Čes Geol úst 75: 229–240

Pašava J, Hladíková J, Dobeš P (1996) Origin of Proterozoic metal-rich black shales from the Bohemian Massif, Czech Republic. Econ Geol 91: 63–79

Pašava J, Kříbek B, Dobeš P, Vavřín I, Žák K, Delian F, Tao Z, Boiron MC (2003) Tin-polymetallic sulfide deposits in the eastern part of the Dachang tin field (South China) and the role of black shales in their origin. Mineral Depos 38: 39–66

Pašava J, Ackerman L, Žák J, Veselovský F, Creaser RA, Svojtka M, Luais B, Pour O, Šebek O, Trubač J, Vosáhlová E, Cividini D (2021) Elemental and isotopic compositions of trench-slope black shales, Bohemian Massif, with implications for oceanic and atmospheric oxygenation in early Cambrian. Palaeogeogr Palaeoclimatol Palaeoecol DOI 10.1016/j.palaeo.2020.110195

Peacor DR, Coveney RM Jr, Zhao GM (2000) Authigenic illite and organic matter: The principal hosts pf vanadium in the Mecca Quarry Shale at Velpen, Indiana. Clays Clay Miner 48: 311–316

Polgári M, Hein JR, Vígh T, Szabó-Drubin M, Fórizs I, Bíró L, Müller A, Tóth L (2012) Microbial processes and the origin of the Úrkút manganese deposit, Hungary. Ore Geol Rev 47: 87–109

Reid AF, Sabine TM, Wheeler DA (1972) Neutron Diffraction and Other Studies of Magnetic Ordering in Phases Based on Cr_2O_3, V_2O_3 and Ti_2O_3. J Solid State Chem 4: 400–409

Rickard D (2019) Sedimentary pyrite framboid size-frequency distributions: A meta-analysis. Palaeogeogr Palaeoclimatol Palaeoecol 522: 62–75

Scharm B, Scharmová M (1995) Accesoric minerals in Proterozoic silexites from Kokšín and Mítov. In: Lysenko Vl. (ed) Results of Enviromental Geological Research in 1996: 21. Odbor ochrany horninového prostředí Ministerstva životního prostředí ČR (in Czech)

Stárková M, Halodová P, Mrázová Š (2018) Origin of Neoproterozoic silicites with stromatolitic structure in the Brdy area. Zpr geol Výzk (Geoscience Research Reports) 51, 1: 57–62. CGS Praha (in Czech)

Strnad L, Mihaljevič M, Šebek O (2005) Laser ablation and solution ICP-MS determination of Rare Earth Elements in USGS BIR-1G, BHVO-2G and BCR-2G glass reference materials. Geostand Geoanal Res 29: 303–314

Wanty RB, Goldhaber MB (1992) Thermodynamics and kinetics of reactions involving vanadium in natural systems: accumulation of vanadium in sedimentary rocks. Geochim Cosmochim Acta 56: 1471–1483

Wignall PB (1994) Black Shales. New York: Oxford University Press, pp 1–127

Xu Hongwu, Guo X, Seaman LA, Harrison AJ, Obrey SJ, Page K (2019) Thermal desulfurization of pyrite: An in situ high-T neutron diffraction and DTA-TGA study. J Mater Res 34: 3243–3253

Yudovich YE, Ketris MP (1994) Trace elements in black shales. Nauka Publisher, Ekaterinburg, pp 1–303 (in Russian)

Zakrzewski MA, Burke EAJ, Lustenhouwer WJ (1982) Vuorelainenite, a new spinel, and associated minerals from the Sätra, central Sweden. Canad Mineral 20: 281–290

Žák J, Svojtka M, Hajná J, Ackerman L (2020) Detrital zircon geochronology and processes in accretionary wedges. Earth Sci Rev 207: 103214